Structural insights into potent inhibition of PDC-3 and PDC-88 β-lactamases by the bicyclic boronic acid inhibitor taniborbactam

Vijay Kumar [1] , Andrew Mack [2] , David A. Six [8] , Krisztina M. Papp-Wallace [1,2] , Robert A. Bonomo [2,3,4,5,6,7] , Focco van den Akker [1]

Department of Biochemistry, Case Western Reserve University School of Medicine, Cleveland, OH, USA [1] ; Louis Stokes Cleveland Department of Veterans Affairs Medical Center, Cleveland, OH, USA [2] ; Department of Medicine [3], Departments of Molecular Biology and Microbiology [4], Pharmacology [5], and Proteomics and Bioinformatics [6], Case Western Reserve University School of Medicine, Cleveland, OH, USA ; CWRU-Cleveland VAMC Center for Antimicrobial Resistance and Epidemiology (Case VA CARES) Cleveland, OH, USA [7] ; Venatorx Pharmaceuticals, Inc., Malvern, Pennsylvania, USA [8].

ABSTRACT

One of the key antibiotic resistance mechanisms in *Pseudomonas aeruginosa* is the expression of chromosomally-encoded *Pseudomonas*-derived cephalosporinases (PDCs) that can hydrolyze β-lactam antibiotics. This PDC family of β-lactamases is continuously expanding with new clinical variants being isolated with so far over 490 members identified. PDC-88 has several amino acid changes compared to one of the most observed PDCs, PDC-3, including a two-residue deletion in the R2 loop in the active site. To probe how the β-lactamase inhibitor taniborbactam (TAN) inhibits these PDC variants, we determined the crystal structure of PDC-3 and PDC-88 in complex with TAN to 1.73 and 1.55 Å resolution, respectively. The electron density in the active sites revealed TAN covalently bound to the catalytic S64 (Ambler residue numbering). One of boronic hydroxyl moieties of TAN makes hydrogen bonds with the backbone nitrogens in the oxyanion hole; the second hydroxyl interacts with Y150. The carboxyl moiety of TAN interacts with T316 and S318; the amide moiety of TAN makes hydrogen bonds across the width of the active site (with the backbone oxygen of S318 and with the side chains of N152 and Q120). The hydrophobic rings in TAN make hydrophobic interactions in the active sites. Overall, our results show that the broad-spectrum β- lactamase inhibitor TAN can be accommodated in the active site of PDC-3 and PDC-88 via numerous hydrogen bonds and hydrophobic interactions, thus explaining its potent inhibition of these PDC variants.

INTRODUCTION

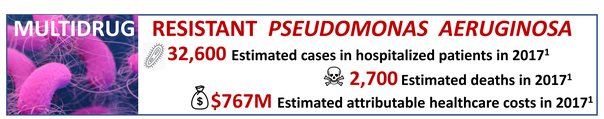

- Multidrug resistance (MDR) in *P. aeruginosa* is classified as a "serious threat" by the CDC, and it causes many types of healthcare-associated infections [1].
- The class C β-lactamases, also known as **AmpC** or **cephalosporinases**, have been known for their large inactivation spectrum, including penicillins, the first cephalosporins (e.g., cephalothin), and cephamycins (e.g., cefoxitin), together with the overall deficiency of inhibition by clavulanic acid, sulbactam, and tazobactam [2].
- *Pseudomonas*-derived cephalosporinase (**PDC**) is the major class C β-lactamase produced by *P. aeruginosa* and is a significant cause of antibiotic resistance.
- PDC-3 and PDC-88 are the variants characterized by a T79A mutation and a T289-P290 amino acid deletion in the R2-loop (Figure 1), respectively [3].
- PDC-88 and other PDC R2-loop deletions reduce susceptibility to cefepime, ceftazidime and ceftolozane-tazobactam [3] .
- Taniborbactam is a novel cyclic boronate β-lactamase inhibitor with activity against all four Ambler classes of β-lactamases [4]. Taniborbactam in combination with cefepime has successfully completed a phase 3 clinical trial.

INTRODUCTION

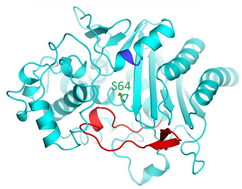

Figure 1. Overall PDC structure (in cyan color) showing the Ω-loop (red) at the entrance of the active site and the T289-P290 (blue) deletion observed in the R2 loop region of PDC-88. The active site catalytic S64 is shown in green stick model representation.

MATERIALS AND METHODS

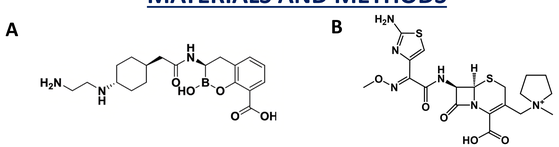

Figure 2. (A) Chemical structure of TAN. **(B)** Chemical structure of cefepime.

RESULTS

MIC and kinetics of PDC-3 and PDC-88 β-lactamases:

A

E. coli strain possessing	Variants	Cefepime MIC (μg/ml) Alone	+ Taniborbactam (4 μg/ml)	+ Avibactam (4 μg/ml)	+ Tazobactam (4 μg/ml)
Vector	-	0.25	0.12	0.12	0.12
PDC-1	-	1	0.25	0.25	1
PDC-3	T79A	2	0.25	0.12	1
PDC-88	T79A, V178L, ΔT289-P290, V329I, G364A	32	0.25	0.25	8

B

	PDC-3			PDC-88		
	K_M (μM)	k_{cat} (s^{-1})	k_{cat}/K_M ($\mu M^{-1} s^{-1}$)	K_M (μM)	k_{cat} (s^{-1})	k_{cat}/K_M ($\mu M^{-1} s^{-1}$)
Nitrocefin	24.7 ± 1.6	720	29.1	53.3 ± 4.6	718	13.5
Cefepime	227 ± 9	0.51 ± 0.04	0.0022 ± 0.0002	26 ± 2	0.15 ± 0.01	0.0058 ± 0.0006

C

	Avibactam		Tazobactam		Taniborbactam	
	K_i (μM)	k_2/K($M^{-1}s^{-1}$)	K_i (μM)	k_2/K($M^{-1}s^{-1}$)	K_i (μM)	k_2/K($M^{-1}s^{-1}$)
PDC-3	2.7 ± 0.3	24,200 ±2,400	27 ± 3	1,200 ± 120	0.66 ± 0.07	160,000 ± 23,000
PDC-88	5.5 ± 0.6	12,000 ± 1,200	58 ± 6	400 ± 40	0.61 ± 0.06	142,600 ± 14,000

Table 1. (**A**) Minimum inhibitory concentrations (MICs) for isogenic *E. coli* expressing PDC β-lactamase constructs. (**B**) A roughly three-fold decrease in turnover (k_{cat}) is countered by a nearly-ten-fold decrease in the Michaelis constant (K_M) to produce an overall three-fold increase in catalytic efficiency (k_{cat}/K_M) for PDC-88 compared to PDC-3. This suggests improved FEP binding plays an important role in the hydrolytic changes. (**C**) Kinetic characterization of the ability of avibactam, tazobactam, and taniborbactam to inhibit PDC. As expected, tazobactam is a kinetically poor inhibitor of PDC. TAN has a lower inhibition constant (K_i) and higher acylation rate (k_2/K) suggesting it more easily forms an acyl-enzyme complex with PDC, but, as shown previously, avibactam has a lower deacylation rate (k_{off}) and longer half-life ($t_{1/2}$) suggesting the complex is more stable [5]. Together, these help to explain why avibactam and TAN are microbiologically indistinguishable with strains expressing PDC [5].

1. Electron density of TAN in active sites of PDC-3 & PDC-88:

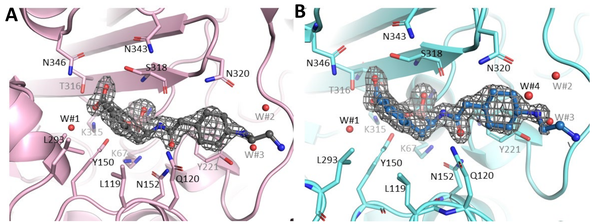

Figure 3. Crystal structures of 1.73 Å PDC-3 and 1.55 Å PDC-88 taniborbactam complexes. Unbiased omit |Fo| - |Fc| electron density map (grey mesh contoured at the 3 σ level) for taniborbactam (in ball-and-stick representation) bound in the active site pocket of (**A**) PDC-3 (light pink color) and (**B**) PDC-88 (aquamarine color). Important active site residues are labelled and shown in stick model, water molecules are also labelled and shown as red spheres. Weaker density for the disordered alkyl-amine tail moiety of taniborbactam indicates its flexible nature.

2. Hydrogen bonding network of TAN in active site:

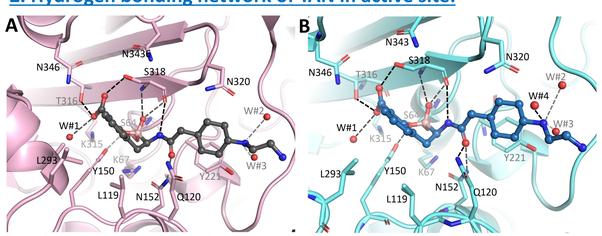

Figure 4. Hydrogen bonding (dashed lines) network of taniborbactam with the active site residues and water molecules in PDC-3 and PDC-88 taniborbactam complexes. (**A**) PDC-3 (light pink) color and (**B**) PDC-88 (aquamarine color). The boron-linked hydroxyl group of taniborbactam engages in hydrogen-bonding interactions with the backbone NH and oxygen of S318 and the second hydroxyl interacts with Y150. The carboxyl moiety of taniborbactam interacts with T316 and S318; the amide moiety of taniborbactam makes hydrogen bonds across the width of the active site (with the backbone oxygen of S318 and with the side chains of N152 and Q120). The cyclohexyl ring of taniborbactam is more distant from the catalytic S64. Three water molecules labelled W#1, W#2 and W#3 also make hydrogen bonds with the taniborbactam.

3. Superposition of apo-PDC-3 and apo-PDC-88 structures:

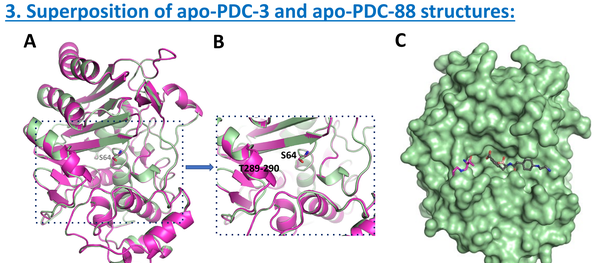

Figure 5. (**A**) Superposition of apo-PDC-3 (light magenta) and apo-PDC-88 (pale green) structures reveals that deletion of T289-P290 residues in PDC-88 leads to the loss of 3_{10} helix in the R2 loop region near the active site (S64 in stick representation). (**B**) Zoomed in view of active site region of (A) shown in dotted rectangle. (**C**) Surface representation of apo PDC-88 (pale green) in the active site pocket (with T289-P290 residues of apo-PDC-3 in stick representation as well as a bound taniborbactam (in ball-and-stick representation with grey carbon atoms) indicating that additional pocket volume at PDC-88's disposal could likely accommodate variable size substrates, and perhaps lead to accelerated release of hydrolyzed products as well.

4. Superposition of apo & TAN bound PDC-3 and PDC-88 structures:

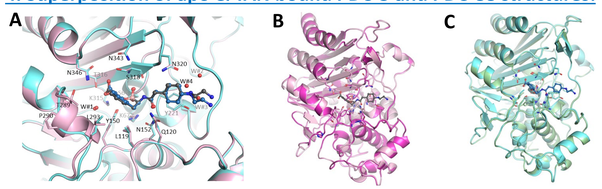

Figure 6. Superpositions of (**A**) active site region of taniborbactam-bound PDC-3 (in light pink color with taniborbactam in ball-and-stick representation with dark grey carbon atoms) and PDC-88 (in aquamarine color with taniborbactam in ball-and-stick with dark blue carbon atoms) structures. (**B**) apo PDC-3 (magenta) and taniborbactam-bound PDC-3 (light pink with taniborbactam in ball-and-stick model), (**C**) overall structure of apo PDC-88 (pale green) and taniborbactam-bound PDC-88 (aquamarine with taniborbactam in ball-and-stick model). Structural superposition reveals that taniborbactam binding and its interactions in the active site region are very similar and the overall fold of the PDC-3 and PDC-88 taniborbactam complexes is also very similar to that of the apo-PDC-3 and apo-PDC-88 structures, respectively.

5. Superposition of TAN bound PDC-3, PDC-88 & $AmpC_{EC}$ structures:

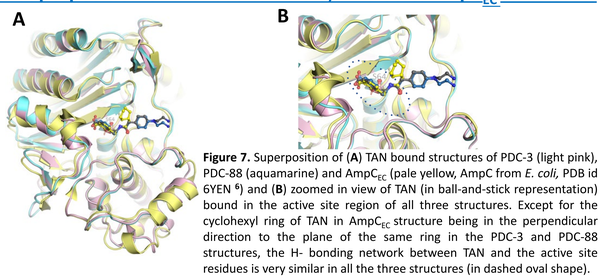

Figure 7. Superposition of (**A**) TAN bound structures of PDC-3 (light pink), PDC-88 (aquamarine) and $AmpC_{EC}$ (pale yellow, AmpC from *E. coli,* PDB id 6YEN [6]) and (**B**) zoomed in view of TAN (in ball-and-stick representation) bound in the active site region of all three structures. Except for the cyclohexyl ring of TAN in $AmpC_{EC}$ structure being in the perpendicular direction to the plane of the same ring in the PDC-3 and PDC-88 structures, the H- bonding network between TAN and the active site residues is very similar in all the three structures (in dashed oval shape).

CONCLUSIONS

- Deletion of T289-P290 residues in PDC-88 variant leads to a loss of 3_{10} helix in the R2 loop region, additional pocket volume near active site of PDC-88's disposal could likely accommodate variable size substrates, and concomitantly with accelerated release of hydrolyzed products in comparison to PDC-3.
- In both complex structures, one of the boronic acid hydroxyl moieties of taniborbactam makes H-bonds with the backbone nitrogen in the oxyanion hole; the second hydroxyl interacts with Y150. The carboxyl moiety of taniborbactam interacts with T316 and S318; the amide moiety of taniborbactam makes H- bonds across the width of active site (with the backbone oxygen of S318 and with the side chains of N152 and Q120).
- Superposition of apo and taniborbactam-bound PDC-3, PDC-88, and $AmpC_{EC}$ structures demonstrates that overall structural fold and active site region is very similar in all three structures, and taniborbactam makes similar hydrogen bonds with the active site residues except that cyclohexyl ring of taniborbactam in $AmpC_{EC}$ structure is perpendicular to the plane of the same ring in the two PDC structures.

REFERENCES

1. Centers for Disease Control and Prevention. (2019) Antibiotic Resistance Threats in the United States, 2019.
2. Philippon A, Arlet G, Labia R, Iorga BI. (2022) Class C β-Lactamases: Molecular Characteristics. *Clin Microbiol Rev*, e0015021.
3. Berrazeg, M. Jeannot, K. Ntsogo Enguéné, VY. Broutin, I. Loeffert, S. Fournier, D. Plésiat, P. (2015) Mutations in β-Lactamase AmpC Increase Resistance of Pseudomonas aeruginosa Isolates to Antipseudomonal Cephalosporins. *Antimicrob Agents Chemother*, 59(10), 6248-55.
4. Hamrick JC, Docquier JD, Uehara T, Myers CL, Six DA, Chatwin CL, John KJ, Vernacchio SF, Cusick SM, Trout REL, Pozzi C, De Luca F, Benvenuti M, Mangani S, Liu B, Jackson RW, Moeck G, Xerri L, Burns CJ, Pevear DC, Daigle DM. (2020) VNRX-5133 (Taniborbactam), a Broad-Spectrum Inhibitor of Serine- and Metallo**β**-Lactamases, Restores Activity of Cefepime in Enterobacterales *and Pseudomonas aeruginosa*. *Antimicrob Agents Chemother*, 64(3):e01963-19.
5. Mack AR, Bethel C, Taracila MA, van den Akker F, Miller BA, Uehara T, Six DA, Papp-Wallace KM, Bonomo RA (2021) 1286. Taniborbactam Inhibits Cefepime-Hydrolyzing Variants of *Pseudomonas*-derived Cephalosporinase (PDC), *Open Forum Infectious Diseases*, Volume 8, Issue Supplement_1, November 2021, Pages S731–S732.
6. Lang PA, Parkova A, Leissing TM, Calvopiña K, Cain R, Krajnc A, Panduwawala TD, Philippe J, Fishwick CWG, Trapencieris P, Page MGP, Schofield CJ, Brem J. (2020) Bicyclic Boronates as Potent Inhibitors of AmpC, the Class C β-Lactamase from *Escherichia coli*. *Biomolecules*, 10(6):899.

ACKNOWLEDGEMENTS

We thank the beamline personnel at National Synchrotron Light Source II (NSLS-II) and Stanford Synchrotron Radiation Lightsource (SSRL) for help with data collection. This project was sponsored by Venatorx Pharmaceuticals, Inc. and funded in part with federal funds from the National Institute of Allergy and Infectious Diseases, National Institutes of Health, Department of Health and Human Services, under Contract No. HHSN272201600029C and Grant 5R44AI109879-04A1.